EINDHOVEN UNIVERSITY OF TECHNOLOGY
Department of Mathematics and Computer Science

CASA-Report 09-33
October 2009

Existence and linear stability of solutions of the ballistic VSC model

by

J. Hulshof, R. Nolet, G. Prokert

Centre for Analysis, Scientific computing and Applications
Department of Mathematics and Computer Science
Eindhoven University of Technology
P.O. Box 513
5600 MB Eindhoven, The Netherlands
ISSN: 0926-4507

Existence and Linear Stability of Solutions of the Ballistic VSC model

J. Hulshof, R. Nolet VU University Amsterdam, G. Prokert, TU Eindhoven

July 3, 2009

Abstract

An equation for the dynamics of the vesicle supply center model of tip growth in fungal hyphae is derived. For this we analytically prove the existence and uniqueness of a traveling wave solution which exhibits the experimentally observed behavior. The linearized dynamics around this solution is analyzed and we conclude that all eigenmodes decay in time. Numerical calculation of the first eigenvalue gives a timescale τ in which small perturbations will die out.

1 Introduction

Tip growth is a process in which single-celled organisms grow roots or hairs, called hyphae, which lengthen at a constant speed, often achieving lengths much larger than their diameters. It is a mechanism by which organisms increase the ratio of surface area to volume probably in order to increase nutrient uptake. Experiments using markers on the cell wall [2] indicate that the wall expands orthogonally to its surface, with growth highly localized in the tip.

The concept of a vesicle supply center (VSC), first proposed by Bartnicki-Garcia *et al* [1], [3], lies at the basis for a whole hierarchy of mathematical models which attempt to explain tip growth. It assumes that there is a point source in the tip which distributes cell wall material for the tip. Vesicles travel from the VSC to the cell wall, producing growth of the cell wall orthogonal to the wall surface. A common result of these models is that the location of the VSC physically coincides with a body called a *Spitzenkörper* within the tip. This body was already suspected to play a role in tip growth.

The ballistic VSC model assumes that vesicles uniformly emanate from the VSC in all directions and travel in straight lines to the cell wall. Bartnicki-Garcia *et al* first derived an analytical expression for the shape of the traveling wave solution for two dimensional cells [1], and later numerically calculated the shape of the three dimensional traveling wave solutions [3]. Koch [9] suggests replacing ballistic motion of the vesicles by a diffusive process. Tindemans [10], [11] has expanded further on this idea and has numerically calculated the shape of the

traveling wave solutions. Other possible modifications of the model include adding elasticity of the cell wall [6], cell wall aging [4] or nonzero absorption times for vesicles [11].

Thus far, all research on VSC type models has focused on numerically determining the shape of the traveling wave solution, little analytical work has been done and no stability results have been proven. In this article we examine the mathematically simplest of the three dimensional models, the ballistic VSC model. We derive a second order parabolic PDE for the evolution of the tip shape and analytically prove the existence, uniqueness and linear stability of the hyphoid solution. We numerically calculate the eigenvalues of the linearized operator, which should give an indication of the timescale in which small perturbations of the cell wall disappear. In a forthcoming paper we intend to combine the approach in this paper with a Schauder fixed point argument to establish the existence of hyphoid solutions for the diffusive VSC model.

The ballistic VSC model is based on the following assumptions:

- The hyphae are rotationally symmetric around the z axis.
- The VSC is located on the z axis and moving at a fixed velocity c. (A stationary VSC would result in a spherical cell)
- Vesicles are emitted uniformly in all direction and travel in straight lines from the VSC to the cell wall where they immediately are absorbed resulting in orthogonal growth. (Whether the VSC produces vesicles or redistributes vesicles produced elsewhere is irrelevant for modeling purposes, in either case we will refer to the total amount surface area added to the cell wall per unit of time as the production rate P of the VSC.)
- The amount of vesicles is large enough that this process can be approximated by a continuous flux of material arriving at the cell wall.

Eggen [4] showed that with these assumptions, the dynamics of the model can be expressed in terms of the mean curvature of the surface, we continue with this idea.

2 The evolution equation

We will model the cell wall as a 2D manifold $M(t)$, axisymmetric around the z axis, star-shaped with respect to the location of the VSC, and embedded in 3D Euclidean space. If we consider the evolution of any piece of the cell wall $A(t) \subset M(t)$, with surface area also denoted as $A(t)$, flowing according to a velocity field $\vec{u}$ defined in a neighborhood of $A(t)$, we have Gauss' formula for the first variation of area:

$$\frac{\mathrm{d}A}{\mathrm{d}t} = -\int_{A(t)} H(\vec{u}\cdot\hat{n})\mathrm{d}A + \oint_{\partial A(t)} (\hat{n}_s\cdot\vec{u})\mathrm{d}s \tag{2.1}$$

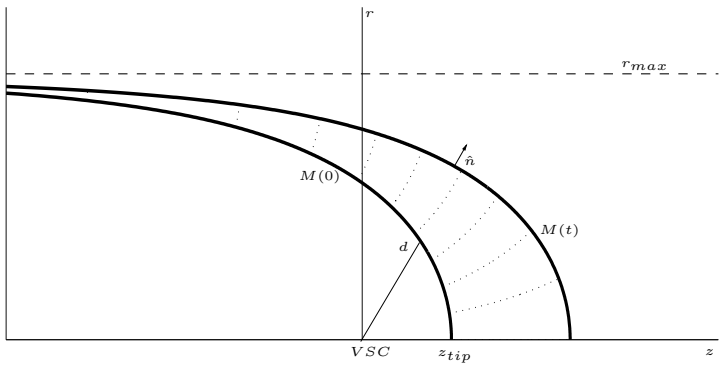

Figure 1: The manifold $M(t)$ and model definitions.

where $\hat{n}$ is the outward pointing normal, $\hat{n}_s$ is the normal to the boundary curve lying in the tangent space of $M(t)$, and H is the mean curvature. Note that, due to our choice of normal, the mean curvature would be negative for a concave surface. We assume the velocity field to be normal to the surface, $\vec{u} = u_n\hat{n}$, the boundary term vanishes and only the integral over u_nH remains.

In the ballistic model, the VSC is moving at constant speed c in the z direction and is assumed to start at the origin at time zero. So its position is $ct\hat{e}_z$. It radiates vesicles in all directions, this can be described by a flux field $\vec{\Phi}$ of the form:

$$\vec{\Phi}(\vec{x}) = \frac{P}{4\pi}\frac{(\vec{x} - ct\hat{e}_z)}{|\vec{x} - ct\hat{e}_z|^3} \tag{2.2}$$

where P is the rate of change of the total area of the manifold, or the production rate of the VSC. The amount of material absorbed in $A(t)$ is:

$$\frac{\mathrm{d}A}{\mathrm{d}t} = \int_{A(t)} (\vec{\Phi}\cdot\hat{n})\mathrm{d}A \tag{2.3}$$

Combining (2.1) and (2.3) to maintain mass balance gives

$$-\int_{A(t)} u_nH\mathrm{d}A = \int_{A(t)} (\vec{\Phi}\cdot\hat{n})\mathrm{d}A \tag{2.4}$$

Since $A(t)$ was chosen arbitrarily, the terms in the integrals must be equal:

$$u_n = -\frac{\vec{\Phi}\cdot\hat{n}}{H}. \tag{2.5}$$

This equation defines a geometric flow which is similar, differing only in the factor $\vec{\Phi}\cdot\hat{n}$, to the inverse mean curvature flow which has been studied extensively by Gerhardt [5], Huisken [7], [8], Urbas [13] and many others. Unfortunately, since we are interested in solutions which are not closed surfaces

and because the flux term $\vec{\Phi} \cdot \hat{n}$ depends not only on the shape of the manifold, but also on the position, it is not clear whether their results and methods can be used for this problem.

The manifold $M(t)$ is embedded in $\mathbb{R}^3$ and we define $F : \Omega \times [0, T) \to \mathbb{R}^3$ for $\Omega \subset \mathbb{R}^2$ to be the embedding map. The manifold is now given by

$$M(t) = \{F(x, t) | x \in \Omega\}, \tag{2.6}$$

here x is a Lagrangian marker of some particle of the cell wall, and $F(x, t)$ gives its location in $\mathbb{R}^3$. The Laplace-Beltrami operator $\Delta_{M(t)}$ on a quantity A is defined as

$$\Delta_{M(t)} A = \frac{1}{\sqrt{g}} \partial_i (\sqrt{g} g^{ij} \partial_j A), \tag{2.7}$$

and a standard result from differential geometry relates the mean curvature vector to the Laplace-Beltrami operator on the embedding map, $H\hat{n} = \Delta_{M(t)} F$. Equation (2.5) can now be written as

$$\frac{\partial F}{\partial t} \cdot \Delta_{M(t)} F = -\frac{P}{4\pi} \frac{\hat{n} \cdot (F - ct\hat{e}_z)}{||F - ct\hat{e}_z||^3}, \tag{2.8}$$

and the condition that the velocity is normal to the surface of the manifold becomes

$$\frac{\partial F}{\partial t} \cdot \partial_i F = 0, \qquad \text{for} \qquad i = 1, 2. \tag{2.9}$$

One now sees that if F satisfies (2.8) with $c = 1$ and $P = 4\pi$, one can scale space and time and substitute

$$\tilde{F} = \frac{P}{4\pi c} F(x, \frac{4\pi c^2}{P} t) \tag{2.10}$$

into (2.8) to see that $\tilde{F}$ solves the equation for arbitrary c and P. So for the rest of this article we shall concern ourselves only with the case $c = 1$ and $P = 4\pi$.

3 Traveling waves

We want to study rotationally symmetric solutions of (2.8) with $P = 4\pi$ and $c = 1$. So $\Omega = I \times S^1$ where I is an interval, $p \in I \subset \mathbb{R}$, and we split F into a radial component $r(p, t)$ and a component in the z direction $z(p, t)$,

$$F(p, \theta, t) = r(p)\hat{e}_r(\theta) + z(p)\hat{e}_z. \tag{3.1}$$

We wish to study traveling wave solutions which move at a speed of one in the z direction. So

$$M(t) = M(0) + t\hat{e}_z. \tag{3.2}$$

In other words, for every p there is an unique q such that

$$F(p, \theta, t) = F(q, \theta, 0) + t\hat{e}_z. \tag{3.3}$$

Each point on $M(t)$ can be seen as a point (with a different coordinate p) of $M(0)$ displaced in the z direction, we define the map $\xi : I \times [0,T) \to I$ which maps p into q as described above. Clearly $\xi(p,0) = p$ and

$$F(p,\theta,t) = F_1(\xi(p,t),\theta) + t\hat{e}_z = r_1(\xi(p,t))\hat{e}_r + (z_1(\xi(p,t)) + t)\hat{e}_z, \tag{3.4}$$

where $F_1(p,\theta) = F(p,\theta,0)$, $r_1(p) = r(p,0)$ and $z_1(p) = z(p,0)$. The curve $(r_1(p), z_1(p)), p \in I$ describes the traveling wave solution in a coordinate frame moving at speed $c = 1$ in the z direction. Physically, if one were to place an ink marker on the fungal hyphae at coordinates (p,θ) at time zero, $F(p,\theta,t)$ would describe how this ink marker would move through space (the dotted curves in Figure 1), in a stationary reference frame the ink marker would appear to move in a direction perpendicular to the cell surface. If, however, one were to move along with the cell tip, the fungal hyphae would appear stationary and $\xi(p,t)$ would describe the p-coordinate of the ink marker as it appears to move backwards along the surface.

3.1 Geometry

We now calculate, using (2.8) and (3.4) some geometric quantities for the manifold $M(t)$. The tangent vectors at coordinates (p,θ) are given by,

$$\begin{aligned} \frac{\partial F}{\partial p} &= \frac{\partial \xi}{\partial p}\left(r_1'(\xi(p,t))\hat{e}_r + z_1'(\xi(p,t))\hat{e}_z\right), \\ \frac{\partial F}{\partial \theta} &= r_1(\xi(p,t))\hat{e}_\theta, \end{aligned} \tag{3.5}$$

and so the metric tensor is

$$g_{ij} = \begin{pmatrix} \left(\frac{\partial \xi}{\partial p}\right)^2 v^2 & 0 \\ 0 & r_1^2 \end{pmatrix}, \tag{3.6}$$

where $v^2 = {r_1'}^2 + {z_1'}^2$. The unit normal is given by

$$\hat{n} = \pm\frac{1}{v}(z_1'\hat{e}_r - r_1'\hat{e}_z), \tag{3.7}$$

where the sign is chosen such that the normal points outward. If the parameter p is such that larger values denote points closer to the tip then the positive sign is chosen. This allows us to write the right hand side of (2.8) as

$$\frac{\hat{n}\cdot(F - t\hat{e}_z)}{|F - t\hat{e}_z|^3} = \pm\frac{1}{v}\frac{z_1'r_1 - r_1'z_1}{(r_1^2 + z_1^2)^{\frac{3}{2}}}. \tag{3.8}$$

The velocity vector is

$$\frac{\partial F}{\partial t} = \frac{\partial \xi}{\partial t}\left(r_1'(\xi(p,t))\hat{e}_r + z_1'(\xi(p,t))\hat{e}_z\right) + \hat{e}_z. \tag{3.9}$$

Since the velocity vector is perpendicular to the tangent vectors,

$$\frac{\partial F}{\partial t}\cdot\frac{\partial F}{\partial p}=\frac{\partial \xi}{\partial p}\left(\frac{\partial \xi}{\partial t}v^2+z_1'\right)=0 \tag{3.10}$$

and we can solve for the time derivative of ξ

$$\frac{\partial \xi}{\partial t}=-\frac{z_1'}{v^2}. \tag{3.11}$$

The mean curvature vector, given by the Laplace-Beltrami operator on the embedding map, is

$$\begin{aligned}\Delta_{M(t)}F&=\frac{1}{r_1 v\frac{\partial \xi}{\partial p}}\left[\frac{\partial}{\partial p}\left(\frac{r_1}{v\frac{\partial \xi}{\partial p}}\frac{\partial F}{\partial p}\right)+\frac{\partial}{\partial \theta}\left(\frac{v\frac{\partial \xi}{\partial p}}{r_1}\frac{\partial F}{\partial \theta}\right)\right],\\&=\frac{1}{r_1 v\frac{\partial \xi}{\partial p}}\frac{\partial}{\partial p}\left(\frac{r_1}{v}(r_1'\hat{e}_r+z_1'\hat{e}_z)\right)-\frac{1}{r_1}\hat{e}_r.\end{aligned} \tag{3.12}$$

We now change to a new variable $\xi=\xi(p,t)$ and use the chain rule, the term $\frac{\partial \xi}{\partial p}$ disappears

$$\Delta_{M(t)}F=\frac{1}{r_1 v}\frac{\partial}{\partial \xi}\left(\frac{r_1}{v}(r_1'\hat{e}_r+z_1'\hat{e}_z)\right)-\frac{1}{r_1}\hat{e}_r, \tag{3.13}$$

and we can write the left hand side of (2.8) as

$$-\frac{\partial F}{\partial t}\cdot\Delta_{M(t)}F=\frac{r_1'}{v}\left(\frac{z_1'r_1''-r_1'z_1''}{v^3}-\frac{z_1'}{r_1 v}\right) \tag{3.14}$$

and (2.8) can be written entirely in terms of the initial manifold, as described by $r_1(\xi)$ and $z_1(\xi)$.

$$r_1'\left(\frac{z_1'r_1''-r_1'z_1''}{v^3}-\frac{z_1'}{r_1 v}\right)=\pm\frac{z_1'r_1-r_1'z_1}{(r_1^2+z_1^2)^{\frac{3}{2}}} \tag{3.15}$$

4 Hyphoid solutions

We call a traveling wave solution which approximates a cylinder of radius r_{max} far away from the tip, a hyphoid solution. In order to study the existence and uniqueness of such hyphoid solutions we choose our parameter p such that it is the z coordinate at time zero, $I=(-\infty,z_{tip})$. So for all p, $z_1(\xi(p,0))=z_1(p)=p$ and clearly $z_1'=1$ and $z_1''=0$. Now since $\frac{\partial}{\partial t}z_1(\xi(p,t))=\frac{\partial \xi}{\partial t}z_1'=\frac{\partial \xi}{\partial t}$ we see that $\xi(p,t)=z_1(\xi(p,t))$. Setting $z=\xi(p,t)$ we can describe our manifold as the graph of a function $r_1(z)$. Using this parametrization (3.15) becomes

$$r_1'\left(\frac{r_1''}{v^3}-\frac{1}{r_1 v}\right)=\frac{r_1-r_1'z}{(r_1^2+z^2)^{\frac{3}{2}}} \tag{4.1}$$

where $v^2 = 1 + r_1'^2$. Multiplying by r_1 we see that this is equivalent to

$$-\frac{\mathrm{d}}{\mathrm{d}z}\left(\frac{r_1}{\sqrt{1+r_1'^2}}\right) = \frac{\mathrm{d}}{\mathrm{d}z}\left(\frac{z}{\sqrt{r_1^2+z^2}}\right). \tag{4.2}$$

Integrating, we get a first order ODE,

$$\frac{r_1}{\sqrt{1+r_1'^2}} = 1 - \frac{z}{\sqrt{r_1^2+z^2}} \tag{4.3}$$

where we have chosen the integration constant such that there is a z_{tip} such that $r_1(z_{tip}) = 0$. If we assume that r_1 has an asymptote $r_1 \to r_{max}$, $r_1' \to 0$ as $z \to -\infty$, we get $r_{max} = 2$ as expected from mass balance.

Solving for the derivative of r_1 gives

$$r_1' = -\sqrt{r_1^2\left(1 - \frac{z}{\sqrt{r_1^2+z^2}}\right)^{-2} - 1} = f(z, r_1). \tag{4.4}$$

This ODE is defined in the region

$$r \geq 1 - \frac{z}{\sqrt{r^2+z^2}} \tag{4.5}$$

outside this region, no traveling wave solutions can exist. Define B to be the lower boundary,

$$B = \left\{(z,r) | r = 1 - \frac{z}{\sqrt{r^2+z^2}}\right\}. \tag{4.6}$$

Solutions which hit B at some point cease to exist to the left of this point. Note that B lies below the line $r = 2$. We will refer to the region below B as the forbidden zone.

Note that we have chosen the negative solution, $r_1' = f(z, r_1) \leq 0$, since we are looking for solutions with $z_{tip} > 0$ and extending in the negative z direction with a positive asymptote $r_1 \to 2$. Choosing the positive square root would result in unrealistic solutions $r_1 < 0$ mirrored over the z axis.

Since any solution is decreasing (and thus solutions above the line $r = 2$ will always stay above this asymptote as $z \to -\infty$), we know that for a hyphoid solution:

$$1 - \frac{z}{\sqrt{r_1^2+z^2}} \leq r_1 < 2 \tag{4.7}$$

4.1 Existence and uniqueness

Theorem 4.1 (Existence and Uniqueness) *There exists a unique hyphoid solution.*

Proof Since a hyphoid solution must lie between the line $r_{max} = 2$ and B, it will pass through a point $(0, x)$ where $x \in (1, 2)$. For $x \in (1, 2)$ let $\gamma_x(z) : I \to \mathbb{R}^+$

be the solution to (4.4) which passes through $(0, x)$, with I the corresponding existence interval.

$$\frac{\mathrm{d}}{\mathrm{d}z}\gamma_x(z) = f(z, \gamma_x(z)), \gamma_x(0) = x. \tag{4.8}$$

We will first examine those values of x for which γ_x is not a hyphoid solution. Let

$$\Sigma^- = \left\{ x \subset (1,2) | \exists z \in (-\infty, 0) : \gamma_x(z) = 1 - \frac{z}{\sqrt{\gamma_x(z)^2 + z^2}} \right\} \tag{4.9}$$

be the set of values of x for which γ_x hits the boundary B of the forbidden zone. Let

$$\Sigma^+ = \{ x \subset (1,2) | \exists z \in (-\infty, 0) : \gamma_x(z) = 2 \} \tag{4.10}$$

be the set of values of x which hits the line $r = 2$. Since the solutions γ_x are ordered, Σ^- and Σ^+ are intervals. For $z^* < 0$ let $\gamma_{z^*}(z)$ be a solution to (4.4) with $(z^*, \gamma_{z^*}(z^*)) \in B$ and let I be the corresponding existence interval. Then $\gamma_{z^*}(z) \leq \gamma_{z^*}(z^*) < 2$ for all $z \in I$ because $r_1' = f(z, r_1) < 0$ outside B and $f(z, r_1) = 0$ if $(z, r_1) \in B$. Consequently $\gamma_{z^*}(z)$ remains bounded and away from B for $z^* < z < 0$, therefore $0 \in I$ and $\gamma_{z^*}(0) \in (1, z^*)$ so $\Sigma^- \neq \emptyset$. In an analogue way one sees that $\Sigma^+ \neq \emptyset$. Straightforward perturbation arguments yield that Σ^+ is an open interval. Finally, the mapping $\Psi : \Sigma^- \to (-\infty, 0)$ given by:

$$\Psi(r) = \Pi_z \left(graph(\gamma_r) \cap B \right), \tag{4.11}$$

with Π_z the projection operator to z, is monotone and maps onto the open interval $(-\infty, 0)$ and thus Σ^- is open. Since $\Sigma^- \subset (1,2), \Sigma^+ \subset (1,2)$ and $\Sigma^- \cap \Sigma^+ = \emptyset$ the set $\Sigma^0 = (1,2) \setminus (\Sigma^- \cup \Sigma^+)$ is closed, not empty and for $x \in \Sigma^0$, γ_x is a traveling wave solution.

We show now that Σ^0 has only one element, otherwise Σ^0 would have interior points. We examine the asymptotic behavior of solutions $\gamma_{\tilde{x}}$ with $\tilde{x}$ in the neighborhood of an interior point x. Differentiating (4.8) with respect to x results in the following linear ODE for $\rho(z) = \frac{\partial}{\partial x}\gamma_x(z)$:

$$\frac{\partial}{\partial z}\rho(z) = \frac{\partial f}{\partial x}(z, \gamma_x(z))\rho(z), \rho(0) = 1, \tag{4.12}$$

where

$$\frac{\partial f}{\partial r}(z, r) = \frac{1}{f}\left(r\left(1 - \frac{z}{d}\right)^{-2} - \left(1 - \frac{z}{d}\right)^{-3}\left(\frac{zr^3}{d^3}\right)\right) \tag{4.13}$$

Since f is negative, negative z implies $\frac{\partial f}{\partial r}(z, r) < 0$ and $\lim_{z \to -\infty} \frac{\partial f}{\partial r}(z, \gamma_x(z)) = -\infty$, so $\rho(z)$ increases exponentially as $z \to -\infty$ and a solution close to γ_x diverges from γ_x as $z \to -\infty$ and so cannot have the same asymptotic behavior. Therefore Σ^0 cannot have interior points and this interval must consist of a single point.

■

4.2 Properties of the hyphoid solution.

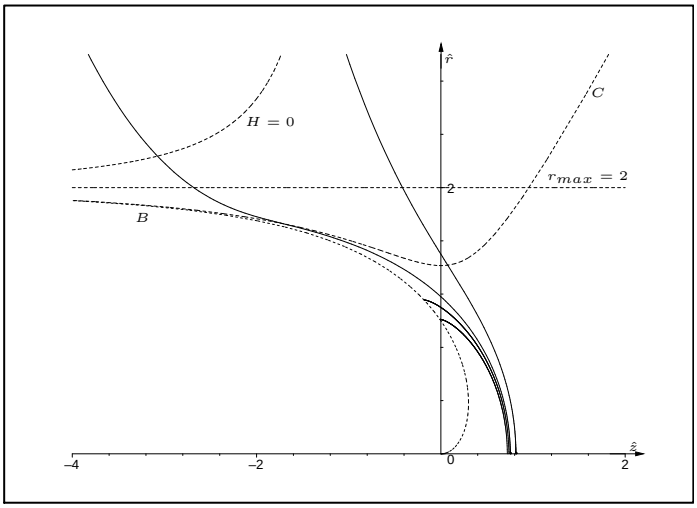

Figure 2: Solid lines: solutions γ_x to (4.8) for $x = 1.01$, $x = 1.1$ in Σ^- and $x = 1.1804$, $x = 1.5$ in Σ^+, Dashed lines: the line $r = 2$, and the curves defined in (4.6), (4.16) and (4.18).

Lemma 4.2 (Properties of the hyphoid solution) *The hyphoid solution has the following properties:*

1. *The tip has no corner.*
2. *The tip is the closest point to the VSC, and is the only extremum of the distance d to the VSC.*
3. *The solution is star-shaped and the mean curvature is strictly negative.*
4. *The solution is concave.*

Proof 1. Tip shape.

Note that if r_1' is finite then the left hand side of (4.4) is $O(r_1)$ as $r_1 \to 0$ while the right hand side is $O(r_1^2)$ for positive z; this yields a contradiction, hence $r_1' \to -\infty$ as $r_1 \to 0$. This means that the tip has no corner.

2. Tip location.

Since the tip has no corner, the distance d to the VSC has an extremum at the tip. If we consider other extrema of the distance, where $d' = \frac{r_1 r_1' + z}{d} = 0$ or $r_1' = -\frac{z}{r_1}$ then, since r_1' is negative, these extrema can only occur if $z \geq 0$. Substituting (4.4) we get an expression for the set of points

(z, r) where $f(z, r) = -\frac{z}{r}$. We show that this curve does not intersect the hyphoid solution. Solving for r gives the trivial solution $r = 0$ and

$$r^2 = 1 - 2z, \qquad 0 \leq z \leq \frac{1}{2} \tag{4.14}$$

This parabola hits the line $r = 0$ at $z = \frac{1}{2}$ and hits the curve B at $(z, r) = (0, 1)$. Differentiating to get the slope m of the tangent to this curve, we get

$$m = -\frac{1}{r} < -\frac{z}{r} = f(z, r) \tag{4.15}$$

so any solution to (4.4) which has an extremum in the distance d other than at the tip, passes through this parabola from left to right and must originate from B. The hyphoid solution does not originate from B and therefore cannot intersect this parabola. So it only has one extremum in d which must be a minimum, the tip is the closest point to the VSC.

3. Star-shapedness.

   For the VSC model to make sense, the hyphoid solution has to be star-shaped with respect to the origin (the location of the VSC) and to have nonzero (and thus negative, due to our choice of normal $\hat{n}$) mean curvature. Since the flux $\vec{F}$ always points away from the VSC, (2.5) says that the two requirements are equivalent. While it is possible to find solutions to (4.3) in which H and $\vec{F} \cdot \hat{n}$ are zero or switch signs, these solutions are physically unrealistic. A solution is not star-shaped with respect to the origin if at any point $r - zr' < 0$. Since r is positive and r' is negative, this can only occur at negative z. We now consider the points where $r - zr' = 0$, combining this with (4.3) and solving for r at negative z one gets:

$$r = 2\frac{z^2}{z^2 - 1} \tag{4.16}$$

   since for $z < -1$ this curve lies above the line $r = 2$, any bounded solution to (4.3), in particular the hyphoid solution, will not cross this curve. Since, for the hyphoid solution, $r - zr'$ is positive at the tip, it is positive everywhere and the hyphoid solution is star-shaped with respect to the origin and has negative mean curvature.

4. Concavity.

   Differentiating (4.4) gives:

$$r'' = \frac{rd^2}{(d-z)^2} - \frac{r^3 z}{(d-z)^3} + \frac{1}{f(z,r)}\frac{r^4}{(d-z)^3} \tag{4.17}$$

   where $f(z, r)$ is given by (4.4). This equation gives the second derivative of r for any traveling wave solution passing through the point (z, r). We now consider the curve C where $r'' = 0$

$$C = \left\{ (z, r) | f(z, r) = \frac{r^3}{r^2 z - d^2(d - z)} \right\}. \tag{4.18}$$

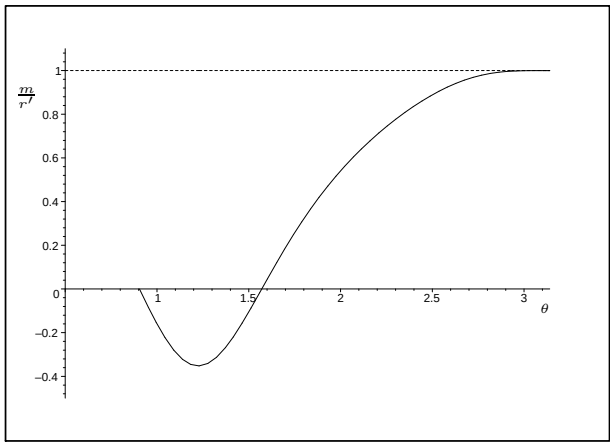

Figure 3: Ratio of the slope m of the curve C to the slope r' of the solution.

We parametrize this curve in polar coordinates $r = \rho(\phi)\sin\phi$, $z = \rho(\phi)\cos\phi$, $d = \rho(\phi)$. Substituting this in the definition (4.4) of f and the equation (4.18) for the curve C we get

$$-\sqrt{\frac{\rho(\phi)^2\sin^2\phi}{(1-\cos\phi)^2} - 1} = \frac{\sin^3\phi}{(1-\cos\phi)(\cos^2\phi + \cos\phi - 1)}. \tag{4.19}$$

Since $f(z,r)$ is negative and $\sin\phi$ is positive, the term $\cos^2\phi + \cos\phi - 1$ on the right hand side must be negative and we see that C stays above the line at angle $\phi_{min} = \arccos(\frac{\sqrt{5}-1}{2})$. Solving for $\rho(\phi)^2$ gives

$$\rho(\phi)^2 = \frac{\sin^4\phi}{(\cos^2\phi + \cos\phi - 1)^2} + \frac{(1-\cos\phi)^2}{\sin^2\phi} \tag{4.20}$$

and

$$C = \left\{(\rho(\phi)\cos\phi, \rho(\phi)\sin\phi) | \phi_{min} < \phi < \pi\right\}. \tag{4.21}$$

If we now examine the slope m of the curve C

$$m = \frac{\frac{\mathrm{d}}{\mathrm{d}\phi}\left(\rho(\phi)\sin\phi\right)}{\frac{\mathrm{d}}{\mathrm{d}\phi}\left(\rho(\phi)\cos\phi\right)} \tag{4.22}$$

and compare this to the slope $r' = f(\rho(\phi)\cos\phi, \rho(\phi)\sin\phi)$ of the traveling wave solution intersecting C we find, using Maple, a symbolic mathematical analysis program, that $\frac{m}{r'}$ has a supremum of 1 as $\phi \to \pi$, so $r' < m$. See also figure 3. So traveling wave solutions cross the curve C from above to below as z increases, and can cross the curve C at most once. The hyphoid solution has $r'' < 0$ in the tip. If the hyphoid solution were

to intersect C, this would imply r'' is positive as $z \to -\infty$ which is in contradiction with the fact that $r' < 0$ and $r' \to 0$ as $z \to -\infty$. So the hyphoid solution cannot intersect C and must be concave. ■

5 Stability of the hyphoid solution

In order to study the stability of the hyphoid solution we consider the manifold to be the graph of the function $z(r,t)$ in a frame of coordinates moving along with the VSC. If a particle p is at radius $r(p,t)$ at time t the embedding map can now be written as

$$F(p,\theta,t) = (z(r(p,t),t) + ct)\,\hat{e}_z + r(p,t)\hat{e}_r. \tag{5.1}$$

As it will be helpful later to consider variations with respect to c, we choose to leave the parameter c in our equations, although we will do all our calculations at $c = 1$. The normal $\hat{n}$ and tangent $\hat{m}$ unit vectors to the manifold are now given by

$$\hat{n} = \frac{1}{v}(\hat{e}_z - z'\hat{e}_r) \qquad \hat{m} = \frac{1}{v}(z'\hat{e}_z + \hat{e}_r) \qquad v^2 = 1 + z'^2. \tag{5.2}$$

Examining the partial derivatives of F we get

$$\begin{aligned} \frac{\partial F}{\partial p} &= r' v \hat{m}, & g_{11} &= r'^2 v^2, \\ \frac{\partial F}{\partial \theta} &= r\hat{e}_\theta, & g_{22} &= r^2, \\ \frac{\partial F}{\partial t} &= \dot{r} v \hat{m} + (\dot{z} + c)\hat{e}_z, & \sqrt{g} &= r' v r. \end{aligned} \tag{5.3}$$

Since $\frac{\partial F}{\partial p} \cdot \frac{\partial F}{\partial t} = 0$ we can solve for $\dot{r}$, and obtain

$$\dot{r} = -\frac{(\dot{z} + c)z'}{v^2}, \qquad \frac{\partial F}{\partial t} = \frac{(\dot{z} + c)}{v}\hat{n}. \tag{5.4}$$

Now the evolution equation (2.8) can be written as a PDE for $z(r,t)$ as

$$\Phi(\dot{z}, z'', z', z, c) = (\dot{z} + c)H - \frac{z'r - z}{(r^2 + z^2)^{\frac{3}{2}}} = 0 \tag{5.5}$$

where the mean curvature H is given by

$$H = \frac{z''}{v^3} + \frac{z'}{rv}. \tag{5.6}$$

In section 4 we showed the existence of an unique hyphoid solution $r_1(z)$ for $c = 1$, since $r_1' < 0$ we can invert this to get a stationary solution $z_1(r)$ to (5.5) at $c = 1$. Using the scaling (2.10) we see that for arbitrary c,

$$z_c(r) = \frac{1}{c} z_1(cr) \tag{5.7}$$

is an equilibrium solution to the PDE, we will require this function in the proof of theorem 5.5.

5.1 The linearized evolution equation

Linearizing around the solution at $c = 1$, $z(r,t) = z_1(r) + w(r,t)$ results in the following linear evolution for w

$$\dot{w} + L[w] = O(w^2) \tag{5.8}$$

with

$$L[w] = a(r)w'' + b(r)w' + c(r)w \tag{5.9}$$

where

$$a(r) = \frac{\partial\Phi}{\partial z''}\Big/\frac{\partial\Phi}{\partial\dot{z}} = \frac{1}{v^3 H}, \tag{5.10}$$

$$b(r) = \frac{\partial\Phi}{\partial z'}\Big/\frac{\partial\Phi}{\partial\dot{z}} = \frac{1}{H}\left(-\frac{3z_1''z_1'}{v^5} + \frac{1}{v^3 r} - \frac{r}{d^3}\right), \tag{5.11}$$

$$c(r) = \frac{\partial\Phi}{\partial z}\Big/\frac{\partial\Phi}{\partial\dot{z}} = \frac{1}{H}\left(\frac{1}{d^3} + \frac{3z_1(z_1'r - z_1)}{d^5}\right). \tag{5.12}$$

Here $d^2 = r^2 + z_1(r)^2$, $v^2 = 1 + z_1'(r)^2$, and H is the mean curvature of the unperturbed surface.

5.2 Divergence form

If we write $w(r,t) = Y(r)\phi(r,t)$ for $Y(r)$ nonzero everywhere, and define the linear operator

$$\tilde{L}[\phi] = \frac{1}{Y}L[Y(r)\phi(r,t)] = a\phi'' + \left(\frac{2aY'}{Y} + b\right)\phi' + \left(a\frac{Y''}{Y} + b\frac{Y'}{Y} + c\right)\phi. \tag{5.13}$$

then, with suitable choices of Y, the operator $\tilde{L}[\phi]$ can be written either in 1D or 2D divergence form. If Y is chosen such that $\frac{2aY'}{Y} + b = a' + \frac{a}{r}$, or

$$\log Y = \int \frac{a' + \frac{a}{r} - b}{2a}\mathrm{d}r \tag{5.14}$$

then $\tilde{L}[\phi]$ is in 2D-divergence form.

$$\tilde{L}[\phi] = -\frac{1}{r}\frac{\partial}{\partial r}\left(r\alpha(r)\frac{\partial}{\partial r}\phi(r,t)\right) + \beta(r)\phi(r,t), \tag{5.15}$$

where

$$\alpha(r) = -a(r), \tag{5.16}$$

$$\begin{aligned}\beta(r) &= a(r)\frac{Y''}{Y} + b(r)\frac{Y'}{Y} + c(r) \\ &= a\left(\frac{\mathrm{d}}{\mathrm{d}r}\left(\frac{a' + \frac{a}{r} - b}{2a}\right) + \left(\frac{a' + \frac{a}{r} - b}{2a}\right)^2\right) + b\left(\frac{a' + \frac{a}{r} - b}{2a}\right) + c.\end{aligned} \tag{5.17}$$

5.3 Asymptotics

One can find formal series solutions for the hyphoid solution $z_1(r)$, its derivatives, and thus for the functions $a(r)$, $b(r)$, $c(r)$, $Y(r)$, $\alpha(r)$ and $\beta(r)$ in the tip as $r \to 0$ and in the asymptote as $r \to 2$. Using standard techniques from asymptotic analysis one can show that these formal series are asymptotic expansions. To first order this gives the following estimates,

$(r \to 0)$	$(r \to 2)$
$z_1 = z_{tip} + O\left(r^2\right),$	$z_1 = -\sqrt{2}(2-r)^{-\frac{1}{2}} + O\left((2-r)^{\frac{1}{2}}\right),$
$z_1' = -\dfrac{1}{2z_{tip}^2} r + O\left(r^3\right),$	$z_1' = -\dfrac{\sqrt{2}}{2}(2-r)^{-\frac{3}{2}} + O\left((2-r)^{-\frac{1}{2}}\right),$
$z_1'' = -\dfrac{1}{2z_{tip}^2} + O\left(r^2\right),$	$z_1'' = -\dfrac{3\sqrt{2}}{4}(2-r)^{-\frac{5}{2}} + O\left((2-r)^{-\frac{3}{2}}\right),$
$H = -\dfrac{1}{z_{tip}^2} + O\left(r^2\right),$	$H = -\dfrac{1}{2} + O\left(2-r\right),$
$a = -z_{tip}^2 + O\left(r^2\right),$	$a = -4\sqrt{2}(2-r)^{\frac{9}{2}} + O\left((2-r)^{\frac{11}{2}}\right),$
$b = -z_{tip}^2 \dfrac{1}{r} + O\left(r\right),$	$b = \sqrt{2}(2-r)^{\frac{3}{2}} + O\left((2-r)^{\frac{5}{2}}\right),$
$c = \dfrac{2}{z_{tip}} + O\left(r^2\right),$	$c = -\dfrac{3\sqrt{2}}{2}(2-r)^{\frac{1}{2}} + O\left((2-r)^{\frac{3}{2}}\right),$
$\log Y = \left(\dfrac{3}{4z_{tip}^2} - \dfrac{1}{4z_{tip}^3}\right) r^2 + O\left(r^4\right),$	$\log Y = \dfrac{1}{16}(2-r)^{-2} + O\left((2-r)^{-1}\right),$
$\alpha = z_{tip}^2 + O\left(r^2\right),$	$\alpha = 4\sqrt{2}(2-r)^{\frac{9}{2}} + O\left((2-r)^{\frac{11}{2}}\right),$
$\beta = \dfrac{3}{z_{tip}} - 3 + O\left(r^2\right),$	$\beta = \dfrac{\sqrt{2}}{16}(2-r)^{-\frac{3}{2}} + O\left((2-r)^{-\frac{1}{2}}\right).$

From these asymptotics we can prove the following properties of α and β.

Lemma 5.1 *Properties of α and β.*

- *α is positive and bounded for all r, near the tip α stays away from zero.*
- *β is bounded near the tip, and is bounded by below by its minimum β_0.*

Proof Positivity of α follows from negativity of H. In the tip $v = 1$, so $\alpha = -\frac{1}{H}$. Since in the tip $z_1' = 0$, from (5.6) we get $H(z_{tip}) = -\frac{1}{z_{tip}^2}$ and so $\alpha(z_{tip}) = z_{tip}^2$. In the asymptote $r \to 2$, $\alpha(r) = O((2-r)^{\frac{9}{2}})$ and so α stays bounded.

From the asymptotics at $r \to 0$ it follows that β is bounded near the tip. From the asymptotics at $r \to 2$ it follows that β is positive and explodes as

$r \to 2$, by continuity it follows that it is bounded from below, we define β_0 to be its minimum. Numerical calculations in Section 6 suggest that $\beta_0 \approx 0.56$ and thus positive, however for now we shall assume nothing about its sign. ■

Corollary 5.2 *$\tilde{L}$ is bounded from below.*

Proof Integrating by parts we obtain,

$$(\tilde{L}u, u)_{L^2} = \int_0^2 (\alpha u'^2 + \beta u^2) r \mathrm{d}r \geq \beta_0 ||u||_{L^2}^2 \tag{5.18}$$

5.4 Eigenvalues of $\tilde{L}[\phi]$

Naively, since in Section 4 we found a class of traveling wave solutions of which the hyphoid solution was a special case, one would expect a zero eigenvalue. However this is not the case. Consider those solutions $r_p(z)$ which cross the line $r = 2$ at the point $(r, z) = (2, p)$. Since $r'(z) < 0$ we can invert these solutions to get functions $z_p(r)$ for $r \in [0, 2]$. If one were to linearize around one such solution at finite p we would certainly get a zero eigenvalue with eigenfunction $\frac{\partial z_p}{\partial p}$. The hyphoid solution can be considered to be the point wise limit of $z_p(r)$ as $p \to -\infty$. Since for $r < 2$ the functions $z_p(r)$ are bounded from below by the hyphoid solution, and since these solutions are ordered, $\frac{\partial z_p}{\partial p}(r) \to 0$. However, by construction, $\frac{\partial z_p}{\partial p}(2) \to 1$. So the pointwise limit as $p \to -\infty$ of the zero eigenfunction. In fact, in this section we will show that all eigenvalues are positive.

We now construct an energetic Hilbert space V as a subspace of $L^2(0, 2)$ with measure $r\mathrm{d}r$ (or equivalently, L^2 on the disc of radius 2 with the standard area measure, restricted to rotationally symmetric functions), and define the Friedrichs' extension of $\tilde{L}$, also denoted as $\tilde{L}$ on V. For more details see Weidmann [14] §5.5.

For test functions $u, v \in C_0^\infty(0, 2)$ the inner product on V is given by

$$\begin{aligned} \langle u, v \rangle_V &= (1 - \beta_0)(u, v)_{L^2} + (\tilde{L}[u], v)_{L^2} \\ &= \int_0^2 (\alpha u' v' + (1 + \beta - \beta_0) uv) r \mathrm{d}r. \end{aligned} \tag{5.19}$$

The space V is the completion of test function under the norm $||u||_V^2 = \langle u, u \rangle_V$. The extended operator $\tilde{L} : D(\tilde{L}) \to L^2$ has a domain dense in V and is self-adjoint on L^2.

Lemma 5.3 *V is compactly embedded in L^2.*

$$V \subset\subset L^2(0, 2) \tag{5.20}$$

Proof By construction, V is continuously embedded in L^2. Now choose a bounded sequence $\{\phi_n\}$ in V. Since $\beta = O((2 - r)^{-\frac{3}{2}})$ there are constants

$A > 0$ and r_0 such that for all $r \in (r_0, 2)$, $1 + \beta(r) - \beta_0 \geq A(2-r)^{-\frac{3}{2}}$. So for positive $\delta \leq 2 - r_0$, if $2 - \delta < r < 2$ then $\frac{1}{A}\delta^{\frac{3}{2}}(1 + \beta(r) - \beta_0) \geq 1$ and

$$\int_{2-\delta}^{2} \phi_n^2 r \mathrm{d}r \leq \frac{1}{A}\delta^{\frac{3}{2}} \int_{2-\delta}^{2} (1 + \beta - \beta_0)\phi_n^2 r \mathrm{d}r \leq \frac{1}{A}\delta^{\frac{3}{2}} ||\phi_n||_V^2. \tag{5.21}$$

and

$$\lim_{\delta \to 0} ||\phi_n||_{L^2(2-\delta,2)} = 0 \qquad \text{uniformly in } n. \tag{5.22}$$

As $\{\phi_n\}$ is bounded in L^2 it has a subsequence, again denoted by $\{\phi_n\}$, which weakly converges to some $\phi \in L^2$. For $k = 1, 2, \ldots$, define $\delta_k \in (0, 1)$ such that

$$\begin{aligned} ||\phi||_{L^2(2-\delta_k,2)} &< \frac{1}{3k}, \qquad \text{and} \\ ||\phi_n||_{L^2(2-\delta_k,2)} &< \frac{1}{3k}. \end{aligned} \tag{5.23}$$

Note that by Lemma 5.1, α and β are well behaved outside the asymptote $r \to 2$, so the sequence of restrictions of ϕ_n to $(0, 2 - \delta_k)$ is bounded in $H^1(0, 2 - \delta_k)$. Due to the compactness of the embedding $H^1(0, 2 - \delta_k) \hookrightarrow L^2(0, 2 - \delta_k)$ (one sees this compactness by considering these spaces with measure $r\mathrm{d}r$ as function spaces on the disc with the usual area measure) we find a subsequence $\{\phi_{n_k}\}$ such that

$$||\phi_{n_k} - \phi||_{L^2(0,2-\delta_k)} < \frac{1}{3k}. \tag{5.24}$$

Hence

$$\begin{aligned} ||\phi_{n_k} - \phi||_{L^2(0,2)} &\leq ||\phi_{n_k} - \phi||_{L^2(0,2-\delta_k)} \\ &\quad + ||\phi_{n_k}||_{L^2(0,2-\delta_k)} \\ &\quad + ||\phi||_{L^2(0,2-\delta_k)} \qquad\qquad < \frac{1}{k}, \end{aligned} \tag{5.25}$$

and we see that the subsequence $\{\phi_{n_k}\}$ converges to ϕ strongly in L^2. ■

Corollary 5.4 *$\tilde{L}$ has a pure point spectrum.*

Proof From Lemma 5.3 this follows directly by Rellich's criterion ([12] Theorem 4.5.3).

Theorem 5.5 Linear stability of the hyphoid solution *All eigenvalues of $\tilde{L}$ are positive.*

Proof We consider variations of the hyphoid solution with respect to the velocity c of the VSC. From (5.5) and (5.7) we know that $z_c(r) = \frac{1}{c} z_1(cr)$ is a solution to $\Phi(0, z_c'', z_c', z_c, c) = 0$. Differentiating by c at $c = 1$ one sees that $L[\frac{\partial z_c}{\partial c}|_{c=1}] + 1 = 0$. Now let $\psi = -\frac{1}{Y}\frac{\partial z_c}{\partial c}|_{c=1} = -\frac{1}{Y}(z_1' r - z_1)$. Since, by Lemma 4.2, the hyphoid solution is star shaped, $z_1' r - z_1 < 0$ and ψ is a positive function. Furthermore $\tilde{L}[\psi] = \frac{1}{Y}$ is positive. Since $\tilde{L}$ is a self-adjoint operator, semi bounded from below, it has a discrete spectrum of eigenvalues

with a smallest eigenvalue λ_1 which can be calculated using the Rayleigh quotient. Let ϕ_1 be a function with $||\phi_1||_{L^2} = 1$ which minimizes $(\phi, \tilde{L}[\phi])_{L^2}$, then λ_1 is this minimum and ϕ_1 lies in its corresponding eigenspace. The absolute value of ϕ_1 also minimizes the Rayleigh quotient, so without loss of generality ϕ_1 may be assumed positive. Now since ϕ_1 is an eigenfunction, $(\psi, \tilde{L}[\phi_1])_{L^2} = (\psi, \lambda_1\phi_1)_{L^2} = \lambda_1(\psi, \phi_1)_{L^2}$, but since $\tilde{L}$ is self-adjoint, $(\psi, \tilde{L}[\phi_1])_{L^2} = (\tilde{L}[\psi], \phi_1)_{L^2} = (\frac{1}{Y}, \phi_1)_{L^2}$. Since $\frac{1}{Y}$, ψ, and ϕ_1 are positive, and the L^2 inner product of two positive functions is positive, the smallest eigenvalue λ_1 must be positive. ■

5.5 Asymptotics of the eigenfunctions

One can find formal series solutions for the eigenfunctions of $\tilde{L}$. Using standard techniques from asymptotic analysis one can show that these formal series are asymptotic expansions. The asymptotic expansion of the eigenfunction ϕ_λ at eigenvalue λ as $r \to 2$ is

$$\begin{aligned} \log \phi_\lambda = &-\frac{1}{16}(2-r)^{-2} - \frac{1}{2}(2-r)^{-1} \\ &+ \sqrt{2}\lambda(2-r)^{-\frac{1}{2}} - \frac{15}{32}\log(2-r) + O\left(\sqrt{2-r}\right). \end{aligned} \tag{5.26}$$

Since $w_\lambda(r) = Y(r)\phi_\lambda$ we can combine this with the asymptotic expansion for Y

$$\begin{aligned} \log Y = &\frac{1}{16}(2-r)^{-2} + \frac{1}{2}(2-r)^{-1} \\ &- \frac{63}{32}\log(2-r) + \frac{57}{32}(2-r) + O((2-r)^2). \end{aligned} \tag{5.27}$$

We see that the first two terms of the expansion cancel out, resulting in the following asymptotic expansion for the eigenfunctions w.

$$w = (2-r)^{-\frac{3}{2}} e^{\sqrt{2}\lambda(2-r)^{-\frac{1}{2}} + O(\sqrt{2-r})}. \tag{5.28}$$

For positive (stable) λ these eigenfunctions increase exponentially as $r \to 2$.

6 Numerical calculations

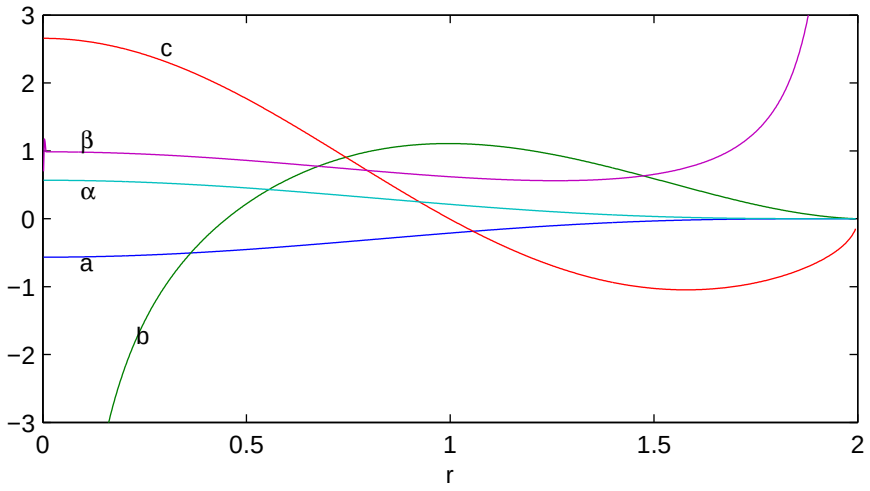

Figure 4: Functions $a(r)$, $b(r)$, $c(r)$, $\alpha(r)$ and $\beta(r)$.

Starting from the second order ODE (5.5) with $c = 1$ and assuming $\dot{z} = 0$ we get a second order ODE in $z(r)$ for the shape of the hyphoid solution. Setting $z_1' = u$ we get the following first order system of differential equations.

$$\frac{\partial}{\partial r}\begin{pmatrix} z_1 \\ u \end{pmatrix} = \begin{pmatrix} u \\ \left(\frac{1+u^2}{r^2+z_1^2}\right)^{\frac{3}{2}}(ur - z_1) - \frac{u}{r}(1+u^2) \end{pmatrix} \tag{6.1}$$

Starting from $r = 1.9951$, $z_1 = -20$ and $u = -2050.3$, as given by the asymptotic expansion as given in Section 5.3 we compute a numerical solution using an initial value solver available in a package such as MatLab. The resulting points (z_1, z_1', r) enables us to calculate higher derivatives using central difference methods and thus we can calculate $a(r)$, $b(r)$, $c(r)$, $\alpha(r)$ and $\beta(r)$. These functions are shown in Figure 4. From these, using finite difference methods and assuming boundary conditions of $\frac{\mathrm{d}\phi}{\mathrm{d}r}(0) = 0$, $\phi(2) = 0$ we can discretize $\tilde{L}$ to obtain a tridiagonal matrix, of which the eigenvalues and eigenvectors can subsequently be calculated.

The five smallest eigenvalues are $\lambda_1 \cdots \lambda_5 = 0.7145, 1.4292, 2.1134, 2.7726,$ and 3.4109, corresponding eigenfunctions are given in Figure 5. Note that it is necessary to calculate the eigenfunctions of the symmetric operator $\tilde{L}$. The eigenfunctions of the operator L are related to these by $w_\lambda = Y\phi_\lambda$ but since the factor Y grows faster than the eigenfunctions decay, the functions w_λ will reach the floating point upper boundary of a computer around $r = 1.9$.

This would imply a generic perturbation will die out at a rate dictated by the first eigenvalue, so with a timescale of $1/\lambda_1 \approx 1.4$. Given a generic hypha

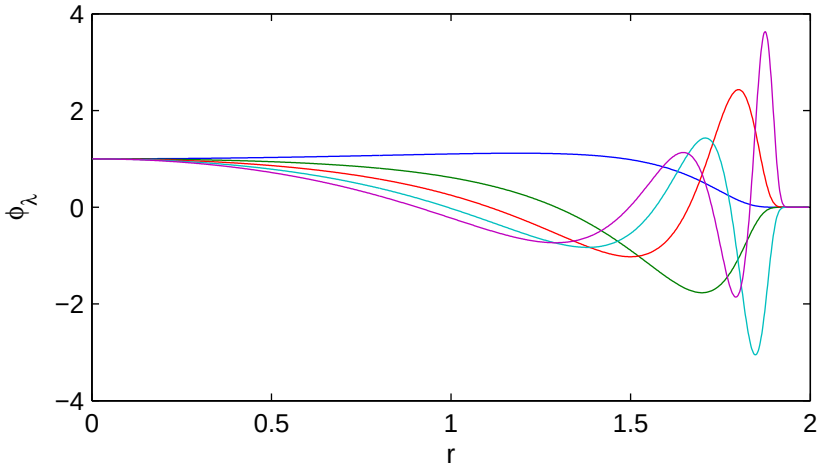

Figure 5: The first five eigenfunctions of the self-adjoint operator $\tilde{L}$.

with production factor P traveling at a velocity c one can use the rescaling described in (2.10) to get the timescale τ in which perturbations die out. (For convenience, using mass balance $P = 2\pi r_{max} c$, we also express τ in terms of the radius r_{max} of the base of the hypha.)

$$\tau \approx 1.4 \frac{P}{4\pi c^2} = 1.4 \frac{r_{max}}{2c} \tag{6.2}$$

7 Conclusions

We have shown that the VSC model has hyphoid solutions, traveling wave solutions similar in shape to fungal hyphae. Moreover, we have shown that these solutions are linearly stable. However, whether this implies nonlinear stability is a nontrivial open problem, especially since the eigenfunctions of L do not decay as $r \to 2$. In this limit the operator degenerates to a transport operator (in coordinates moving along with the tip) and a perturbation away from the tip will move further down the asymptote without decaying. It should however be possible, when restricting ourselves to a compact area near the tip, to show that perturbations do decay at a rate dictated by the first eigenvalue. We intend to discuss this in a forthcoming paper.

Acknowledgments

We would like to thank the group of Bela Mulder at the AMOLF for suggesting this problem and for useful discussions.

References

[1] Bartnicki-Garcia, S., Hergert, F., Gierz, G. : Computer simulation of fungal morphogenesis and the mathematical basis for hyphal (tip) growth, Protoplasma 153, 46-57 (1989)

[2] Bartnicki-Garcia, S., Bracker, C.E., Gierz, G., Lopez-Franco, R., Lu, H. : Mapping the growth of fungal hyphae: orthogonal cell wall expansion during tip growth and the role of turgor. Biophys. J. 79, 2382-2390 (2000)

[3] Bartnicki-Garcia, S., Gierz, G. : A Three-Dimensional Model of Fungal Morphogenesis Based on the Vesicle Supply Center Concept, J.Theor.Biol. 208, 151-164 (2001)

[4] Eggen, E. : Master's Thesis, Self-Regulating Tip Growth, Modeling Cell Wall Ageing, http://www.phys.uu.nl/~veg/thesis/thesis.pdf (2006)

[5] Gerhardt, C. : Flow of Nonconvex Hypersurfaces into Spheres, J. Diff Geom. 32, 299-314 (1990)

[6] Goriely A., Tabor M. : Self-similar tip growth in filamentary organisms. Phys. Rev. Lett. 90, 108101 (2003).

[7] Huisken, G., Ilmanen T. : A Note on the Inverse Mean Curvature Flow, Proc. Workshop on Nonl. Part. Diff. Equ. (Saitama University, Sept. 1997), available from Saitama University, also http://www.math.nwu.edu/~ilmanen (1997)

[8] Huisken, G., Ilmanen T. : Higher Regularity of the Inverse Mean Curvature Flow, http://www.math.ethz.ch/~ilmanen/papers/pub.html (2002)

[9] Koch, A. : The problem of hyphal growth in streptomycetes and fungi, J.Theor.Biol. 171, 137-150 (1994)

[10] Tindemans, S. : Master's Thesis, Modeling Tip Growth in Fungal Hyphae (2004)

[11] Tindemans, S., Kern, N., Mulder, B. : The diffusive vesicle supply center model for tip growth in fungal hyphae, J. Theor. Biol. 238, 937-948 (2006)

[12] Triebel, H. : *Higher Analysis*, Barth Leipzig/Berlin/Heidelberg (1992)

[13] Urbas, J. : On the expansion of starshaped hypersurfaces by symmetric function of their principal curvatures, Math. Z. 205, 355-372 (1990)

[14] Weidmann, J. : *Linear Operators in Hilbert Spaces*, Springer-Verlag Graduate Texts in Mathematics, (1980)

PREVIOUS PUBLICATIONS IN THIS SERIES:

Number	Author(s)	Title	Month
09-29	R. Ionutiu J. Rommes	Model order reduction for multi-terminal circuits	Sept. ‘09
09-30	M. Günther G. Prokert	Existence of front solutions for a nonlocal transport problem describing gas ionization	Sept. ‘09
09-31	G. Díaz J. Egea S. Ferrer J.C. van der Meer J.A. Vera	Relative equilibria and bifurcations in the generalized van der Waals 4-D oscillator	Sept. ‘09
09-32	J.H.M. ten Thije Boonkkamp M.J.H.Anthonissen	Extension of the complete flux scheme to time-dependent conservation laws	Sept. ‘09
09-33	J. Hulshof R. Nolet G. Prokert	Existence and linear stability of solutions of the ballistic VSC model	Oct. ‘09

Ontwerp: de Tantes,
Tobias Baanders, CWI